Molecular Manipulation of Micro-Environment of Au Active Sites on Mesoporous Silica for Enhanced Catalytic Reduction of 4-Nitrophenol

Meng Ding,[a] Bo Peng, *,[a] Jia-Feng Zhou,[a] Hui Chen, [a] Yi-Song Zhu,[a] En-Hui Yuan,[e] Belén Albela,[b] Laurent Bonneviot,[b] Peng Wu,[a,d] Kun Zhang*, [a,b,c,d]

[a] Shanghai Key Laboratory of Green Chemistry and Chemical Processes, College of Chemistry and Molecular Engineering, East China Normal University, Shanghai 200062, China;

[b] Laboratoire de Chimie, Ecole Normale Supérieure de Lyon, Institut de Chimie de Lyon, Université de Lyon, 46 Allée d'italie, Lyon 69364 CEDEX 07, France;

[c] Shandong Provincial Key Laboratory of Chemical Energy Storage and Novel Cell Technology, School of Chemistry and Chemical Engineering, Liaocheng University, Liaocheng, Shandong 252059, P. R. China;

[d] Institute of Eco-Chongming, Shanghai 202162, China;

[e] Key Laboratory of Syngas Conversion of Shaanxi Province, School of Chemistry & Chemical Engineering, Shaanxi Normal University, Xi'an, 710119, China;

Bo Peng (BP): Email: bpeng@chem.ecnu.edu.cn; Kun Zhang (KZ): Email: kzhang@chem.ecnu.edu.cn

Abstract

At the confined nanospace and/or nanoscale interface, the catalytic nature of active sites on the molecule level still remains elusive. Herein, with the catalytic hydride reduction of 4-nitrophenol (4-NP) over gold nanoparticles (NPs) catalysts as a prototype reaction, the influence of delicate change of microenvironment of catalytic active site on the reaction kinetics of 4-NP to 4-aminophenol (4-AP) with the introduction of varied alkali-metal ion (AM^+) salt, have been deeply investigated. We demonstrate that structural water (SW) adsorbed on Au NPs in the form of {$OH^-\cdot H_2O$@Au NPs} is the real catalytic active sites (not alone Au NPs), and in the presence of lithium chloride (LiCl), it shows the best catalytic performance. In addition, the isotope labeling and kinetic isotope effect (KIE) experiments evidences that, the reduction of 4-NP does not follow the classical Langmuir-Hinshelwood (L-H) bimolecular mechanism, but an interfacial SW dominated electron and proton transfer mechanism. The proposed mechanism answers why the dissociation of O-H bond of water is the rate-determining step (RDS) of 4-NP reduction, and, counter-intuitively, the solvent water is the hydrogen source of final product 4-AP, instead of sodium borohydride ($NaBH_4$) reducer. Importantly, the co-existence of Li^+ and Cl^- ions synergistically stabilizes the transition state of reaction and accelerates the interfacial electron and proton transfer, consequently enhancing the reaction kinetics. The model of structural water as a bridge to transfer electron and proton at nanoscale interface is the reminiscent of working mechanism of photosystem two (PSII) for water splitting on Mn_4CaO_5 cluster.

Introduction

Over the past several decades, the reduction of 4-nitrophenol (4-NP) to 4-aminophenol (4-AP) by sodium borohydride ($NaBH_4$) has become a benchmark or model reaction to assess the catalytic activity of metal nanoparticles (NPs) in aqueous media.[1-6] The well accepted reaction mechanism of metal NPs-catalyzed 4-NP

reduction is based on the Langmuir-Hinshelwood (L-H) bimolecular adsorbed model,[7-9] where two reactants of 4-NP and $NaBH_4$ adsorb on the surface of metal NPs before the reaction. Obviously, the hydrogen source of 4-AP final product could be coming from $NaBH_4$ reducer. However, it is not the case, isotope labeling experiments with $NaBD_4$ and D_2O verified that the hydrogen source of 4-AP is counter-intuitively originated from the water solvent, instead of $NaBH_4$ reducer.[10-13] In addition, based on the L-H mechanism, noble metals are necessary because they act as both the adsorption center of the reaction substrate and the electron transfer medium.[8, 14-24] However, very recently, there are many examples of catalysts shows that the catalytic efficiency is not only attributed to the metal NPs center, but also to the microenvironment around metal catalysts, such as the pH, the type of solvent and the ion additives.[10, 11, 25-31] For example, even in the absence of metal catalysts, both N-doped graphene[32] and surfactant aggregate[33] catalysts showed high chemical reactivity for the selective reduction of 4-NP to 4-AP, triggering the debate whether noble metal nanoparticles are the catalytic active sites for this reaction. Thus, even as listed one of the widely investigated benchmark reaction, the underlying reaction mechanism of 4-NP at nanoscale interface is not clear.

Herein, using mesoporous silica nanoparticles with a unique dendritic structure (DMSNs) as a support, highly dispersed gold NPs catalyst in size of *ca.* 2.4 nm was synthesized. With the catalytic reduction of 4-NP as a probe reaction, we systematically investigated the effect of alkali metal cations (AM^+) and its counter-anions on the reaction kinetics of the reduction of 4-NP in an aqueous $NaBH_4$ solution. We demonstrated that the reaction kinetics are strongly dependent on the type and concentration of used alkali metal salts. When the counter-anion is Cl^-, the introduction of Li^+ significantly accelerates the reaction rate, and with the increase of radius of AM^+, the reaction rate is decreased in order of $Li^+ > Na^+ > K^+ > Rb^+ > Cs^+$. Very interestingly, the designed experiments of isotope labeling and kinetic isotope effect (KIE) with $NaBD_4$ and D_2O proved that, water is the hydrogen source of 4-AP, instead of sodium borohydride ($NaBH_4$) reducer, and the dissociation of O-H bond of water is the rate-determining step (RDS). In addition, combined with the characterizations of optical spectrum, we identified that structural water (SW) adsorbed on the Au NPs in the form of {$OH^-\cdot H_2O$@Au NPs} is the catalytic active site for the reduction of 4-NP as a whole, not alone Au NPs. Due to the spatial overlaps of the p orbital of oxygen atoms of SW at confined nanoscale interface, an ensemble of interfacial electronic states is produced, which provides alternative channels for surface electron and proton transfer. The presence of Li^+ with strong hydration capacity probably stabilizes the transition state of the reaction intermediate by H-bond interaction, which accelerates the dissociation of O-H bond in water and concurrently the cleavage of N-O bond in 4-NP, resulting in the enhanced reaction kinetics of 4-NP reduction.

Result and discussion

Dendritic mesoporous silica nanoparticles supported gold nanoparticles catalyst (Au@DMSNs) was prepared by a multi-step in situ nanocrystal seeding induced growth (SIG) method with sodium borohydride ($NaBH_4$) as reducer and amino-functionalized DMSNs as a unique confinement support (Fig. 1a and Experimental details in the

Supporting Information).[34] Note that the grafting of amino group and the nested spherical pore in the dendritic network of DMSNs can provide both chemical and physical confinement effect on the gold NPs (Fig. 1a).[35-38] The combined characterization by the X-ray diffraction (XRD) (Fig. 1b) and transmission electron microscopy (TEM) (Fig. 1c) confirmed that highly dispersed Au NPs (~2.4 nm) were encapsulated into the pores of DMSNs. ICP-OES analysis indicated the actual loading amount of Au was 1.18 wt% (Table S1), which is consistent with the previous work,[24] and the real loading weight was less than the feeding ratio of 2%, implying partial leaching of metal during the synthesis of catalysts. The XPS spectrum of Au 4f for Au@DMSNs catalysts was deconvoluted into Au^0 and $Au^{\delta+}$ two components with binding energies of 83.0 eV and 84.5 eV, respectively (Fig. S1), and the content of Au^0 accounts for a large fraction up to ~78% to all Au atoms (Table S2). Besides, the binding energy of dominant Au^0 (83.0 eV) species was lower than that of the standard crystalline Au (84.0 eV), featuring the negative valence state of gold NPs confined in the nanopores of DMSNs. The striking negative valence state of Au NPs was assigned to the favorite adsorption of the hydrous hydroxyl (or hydrous hydroxide) groups with negative charges on the large number of the coordinatively unsaturated Au atoms (Fig. 1a, zoom in analysis),[39-43] which is also called interfacial structural water molecules (SW).[44-47]

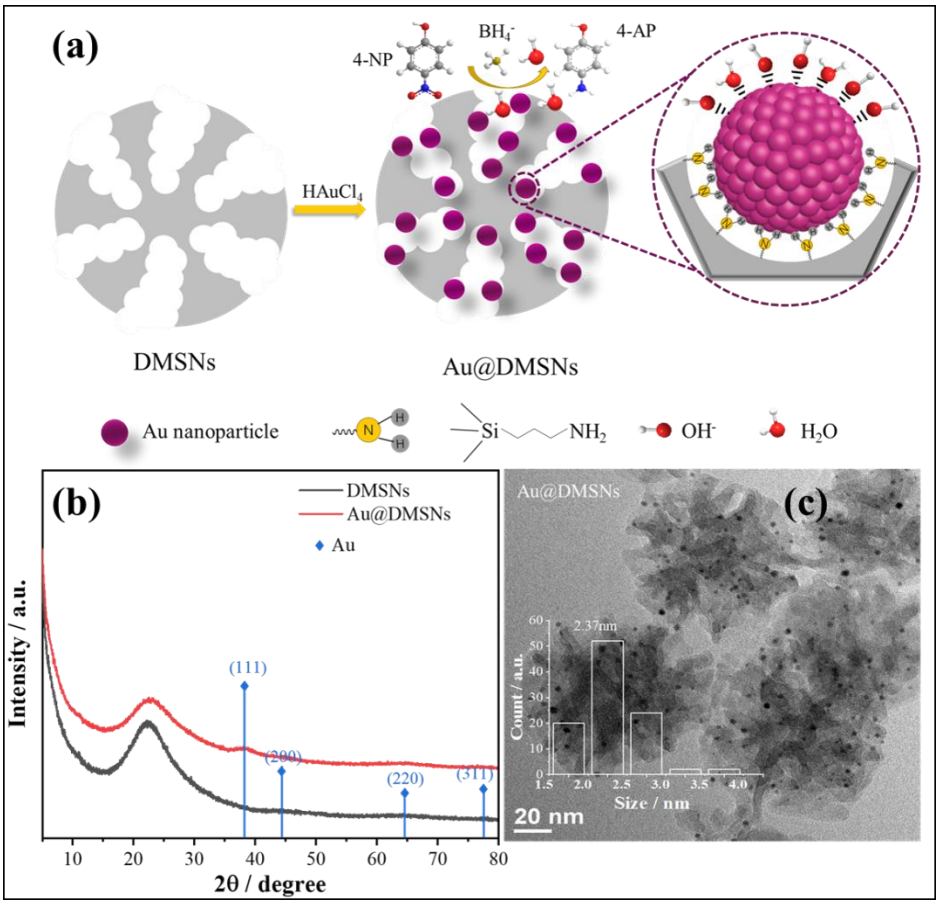

Figure 1. Schematic illustration of the synthesis procedure of Au@DMSNs catalysts (a) and its characterizations by XRD (b) and TEM (c).

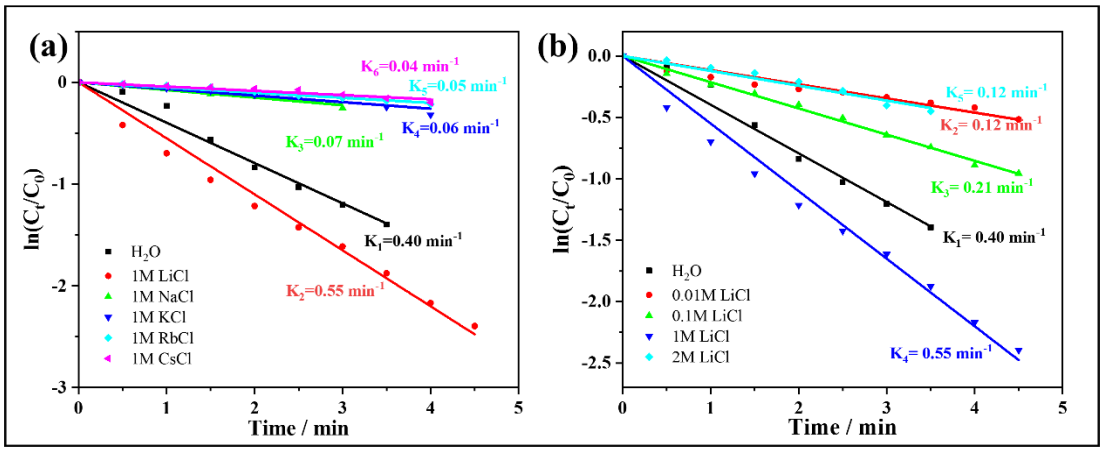

Figure 2. Catalytic activity of Au@DMSNs catalysts for the reduction of 4-NP in the different alkali-metal chloride (AMCl, AM= Li, Na, K, Rb, Cs, 1 M) aqueous solution (a) and the aqueous solution with different concentration of LiCl (b). K_n is the apparent pseudo-first-order rate constant as the molar ratio of $NaBH_4$/4-NP was about 200 in the reaction.

The catalytic activity of Au@DMSNs catalyst for the reduction of 4-NP to 4-AP was tested in the aqueous $NaBH_4$ solution with the introducing of a series of alkali metal chloride (1 M). As shown in Fig. 2a, the catalytic activity was strongly dependent on the type of alkali metal cations, the rate constant (k) increased with the order of Cs^+ (0.04 min^{-1}) < Rb^+ (0.05 min^{-1}) < K^+ (0.06 min^{-1}) < Na^+ (0.07 min^{-1}) < Li^+ (0.55 min^{-1}), and only the catalytic activity with the introducing of Li^+ (0.55 min^{-1}) surpassed the intrinsic activity of Au@DMSNs catalysts in water (0.40 min^{-1}). Besides, the catalytic activity showed a volcano-type trend with the concentration of LiCl (0.01-2 M), the rate constant (k) firstly increased from 0.12 min^{-1} to 0.55 min^{-1} and then decreased to 0.12 min^{-1} with the concentration of LiCl increased from 0.01 M to 1 M and then to 2 M, in which reach a maximum in 1 M LiCl aqueous solution (Fig. 2b). In most of cases, it was accepted that the introducing of metal cations into $NaBH_4$ could alter the reducing power of BH_4^-,[48-50] whereas, it can hardly account for the observed trend in the rate constants. In fact, the counter ions of lithium also showed a significant impact on the catalytic activity (Fig. S2). when the counter ion Cl^- of Li^+ was replaced by NO_3^-, the reaction rate was decreased to 0.14 min^{-1}; surprisingly, when the substituted anions are Br^-, I^-, and SO_4^{2-}, the Au@DMSNs catalyst almost lost the reactivity, suggesting that the reaction kinetics of the reduction of 4-NP is extremely sensitive to the delicate change of micro-environment of catalytic active sites.[30, 51, 52]

To further elucidate the reaction micro-kinetics of the alkali metal cation-dependent catalytic activity on the molecule level, kinetic isotope effects (KIEs) and isotope labelling experiments were performed to determine the rate-determining steps of the reduction of 4-NP.[7-9] As shown in Fig. 3a and 3b, the KIEs values of Au@DMSNs catalysts in water are 2.76 and 1.59 for solvent ($K_{H2O/D2O}$) and reagent ($K_{NaBH4/NaBD4}$), respectively, which indicated that the dissociation of the B-H/B-D bond of BH_4^-/BD_4^- and O-H/O-D of H_2O/D_2O are both involved in the reduction reaction,[10-13] and the much larger KIE value of solvent water (2.76) compared to that of reducer $NaBH_4$ (1.59) suggests that the reaction-determining-step (RDS) in the reduction of

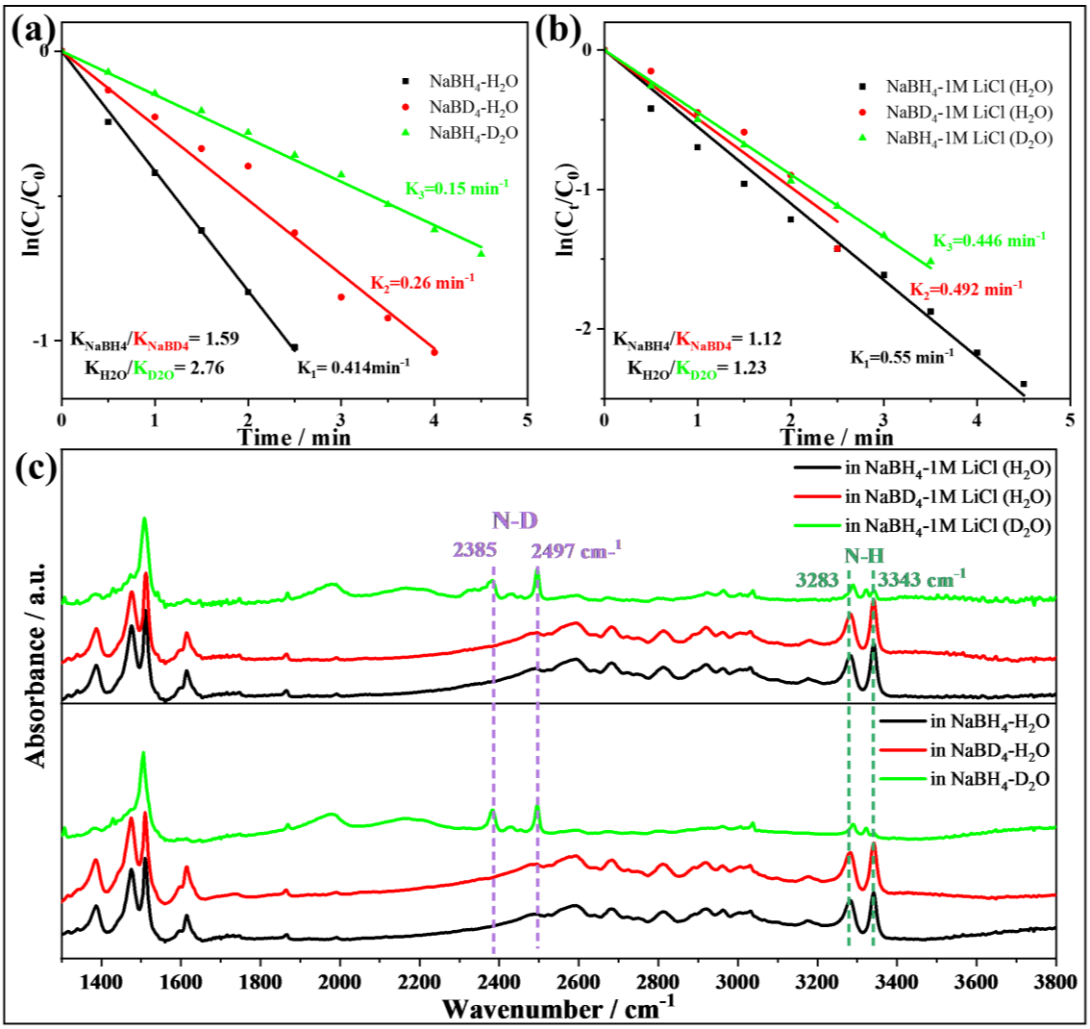

Figure 3. Kinetics isotope effects (KIE) of reagent ($NaBH_4$/$NaBD_4$) and solvents (H_2O/D_2O) in the reduction of 4-NP on Au@DMSNs using water (a) and 1 M LiCl aqueous solution (b) as reaction media. (c) FTIR spectra of the final products after the reduction of 4-NP on Au@DMSNs using 1 M LiCl aqueous solution (top) and water (bottom) as reaction media and $NaBH_4$ and H_2O (black line), $NaBD_4$ and H_2O (red line), and $NaBH_4$ and D_2O (green line) as reducer and solvent, respectively.

4-NP is the cleavage of O-H bond of water rather than the cleavage of B-H bond of $NaBH_4$. Notably, when LiCl aqueous solution (1 M) was introduced into reaction system, both the reagent ($K_{NaBH4/NaBD4}$) and solvent ($K_{H2O/D2O}$) KIE value are approximately equal to 1 (1.12 for $K_{NaBH4/NaBD4}$ and 1.23 for $K_{H2O/D2O}$), suggesting that the introducing of LiCl further stabilized the transition state of reaction intermediate species probably by H-bond interaction, consequently further accelerating the reaction kinetics by the activation of O-H bond of water.

The isotope labelling experiments further emphasized the vital role of water in the hydride reduction of 4-NP with Au@DMSNs as catalysts, the deuterium isotope labelled reduction products by D_2O or $NaBD_4$ were obtained from the large-scale catalytic reaction system with the combination of reducer and solvent as $NaBH_4 + H_2O$, $NaBD_4 + H_2O$ and $NaBH_4 + D_2O$, respectively. The FT-IR spectra of commercial 4-NP

and 4-AP (Fig. S3) and as-obtained products (Fig. 3c) in the reaction media of water and 1 M LiCl aqueous solution were recorded, the absorption peaks centered at about 3283 and 3343 cm^{-1} are attributed to the stretching modes of N-H bond (Fig. 3c, olive dash line),[11, 26] and the absorption peaks centered at about 2385 and 2497 cm^{-1} are attributed to the stretching modes of N-D bond (Fig. 3c, purple dash line).[11] Intriguingly, no matter the reaction media is water or 1 M LiCl aqueous solution, the stretching modes of N-D bond can be only observed in the reaction system of $NaBH_4$ + D_2O rather than the reaction system of $NaBD_4$ + H_2O, suggesting that the hydrogen source of products was originated from water rather than reducer $NaBH_4$. Thus, the isotope labelling experiments provide the solid evidences that, surface adsorbed water directly involves the interfacial electron and proton transfer for selective reduction of 4-NP, which does not follow the classical L-H mechanism. However, the structure of interfacial water and how it manipulates electrons and protons at the nano-confined interface are not clear.

Very recently, after long-term and systematic research on the physical origin of the bright photoluminescence (PL) of noble metal nanoclusters,[53-56] we identified that water molecules (namely structural water molecules, SW) adsorbed or confined at the nanoscale interface could form a new interfacial state with the characteristics of a conjugated π-bond (namely p band intermediate or transient state, PBIS) due to the spatial overlap of *p* orbitals of oxygen atoms in SW (Fig. S4), which could emit bright color and act as alternative reaction channel for static electron transfer.[12, 13, 30, 39, 44-47, 57] Using this model, we clearly answered the physical origin of water as bright emitters for photoluminescence (PL), finishing a century of debate on this issue.[58, 59] Thus, we suppose that, if the interfacial SW involves the construction of Au NPs catalytic active sites, the optical spectrum will show clear evidences. As shown in Fig. 4a, when the Au@DMSNs catalyst was dispersed in the aqueous solution, it showed a strong emission peak centered at 425 nm with main excitation bands centered at 355 nm with a should peak at 290 nm (Fig. 4a, black line), which is assigned to structural water (SW), stemming from p band intermediate state with the characteristics of π-bonding due to

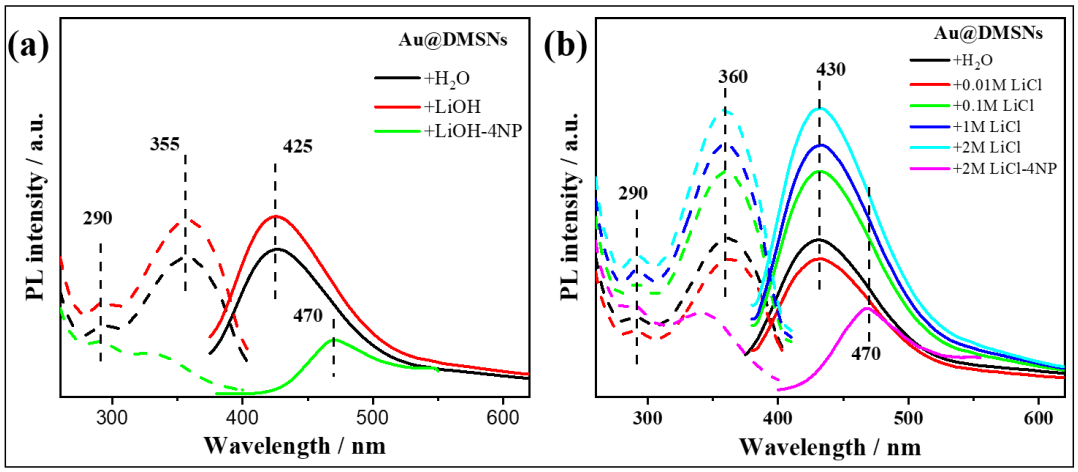

Figure 4. Excitation (dot line) and emission (solid line) spectra of Au@DMSNs catalysts in 1 M LiOH aqueous solution (a) and the aqueous solution with different concentration of LiCl (b) before and after the addition of 4-NP.

the spatial overlap between the *p* orbitals of oxygen atoms of SW.[44, 45] Besides, we interestingly found that, upon the addition of lithium hydroxide (LiOH), the PL intensity was slightly increased, but the position at 425 nm did not show any shifts, (Fig. 4a, red line), suggesting the enhanced stability and/or increased number of SW at nanoscale interface, consistent with the structure of SW in the form of {$OH^-·H_2O$@Metal}.[44, 45, 47] Importantly note that, if the excessive introduction of LiOH is not conducive to 4-NP reduction, because the over-saturated adsorption of OH^- ions on the Au NPs surface will compete for the adsorption of reactants with the same negative charge (BH_4^- and 4-NP), thus quenching the reaction (Fig. S5). This observation also answered our previous result that, only at medium concentration of NaOH solution, the reduction of 4-NP exhibited the highest chemical reactivity at Ag NPs based catalysts.[30]

Interestingly, when the reagent 4-NP was added, the emission band is red-shifted from 425 nm to 470 nm with a dramatical dcreased intensity, the excitaion band at *ca.* 355 nm was blue-shifted to *ca.* 340 nm (Fig. 4a, green line). This suggests that 4-NP substrate involves the contructing of a new interface state by *p* orbital interaction of O and N atoms of 4-NP with structural water (SW), forming a hyperconjugation by space interaction at nanoscale interface. Obviously, it is not easy to maintain the hyperconjugation of multiple atoms at the nanoscale interface at the same time. This also answers why the PL emission intensity of the Au NPs catalyst is significantly reduced after the introduction of 4-NP (Fig. 4a, green line), and the reaction kinetics of 4-NP reduction is extremely sensitive to any delicate change of the microenvironment of the catalytic active sites, such as type and concentration of alkali metal ions (Fig. 2) and its counter ions (Fig. S2). In addition, it is worthy noting that, when Au@DMSNs was dispersed in the LiCl aqueous solution, PL intensity at 430 nm was increaesd with the increase of concentration of LiCl solution (Fig. 4b), suggesting that the introdction of LiCl favours the stablization of the interface state of structural water and/or raises up the numbers of SW. Thus, with the characterizations of the optical spectrum, we clearly confirmed that structural water (SW) adsorbed on the Au NPs in the form of {$OH^-·H_2O$@Au NPs} could form some alternative interface states (or channels) for sufrace elcetron transfer (or decay) due to the overlapping of *p* orbitals by space interaction.

Combining the characterization of the optical spectrum with the data of reaction kinetics with isotope labeling, a simple model with SW adsorbed on Au NPs in the form of {$OH^-·H_2O$@Au NPs} as catalytic active sites was proposed to explain the alkali metal cation- and its anion-dependent catalytic activity of the benchmark or model reaction-hydride reduction of 4-NP (Scheme 1) where SW as a bridge to connect the reaction substrate BH_4^- (electron donor) and 4-NP (electron acceptor) for surface long-range electron transfer by the spatial overlaps of *p* orbitals of one B atom in BH_4^-, two oxygen atoms in SW and one O atom in 4-NP.[39, 44, 45, 55, 60, 61] Obviously, the transition state of reaction intermediate composed of multiple atoms by space interaction of their *p* orbitals is unstable and easily affected by the delicate change of microenvironment of catalytic active center, for example, type and concentration of AM^+ and its counter anion. In the aqueous $NaBH_4$ solution (pH = *ca.* 8.4), the negatively charged surface of

Au@DMSNs catalysts are compensated by the electro-neutrality due to the electrostatic

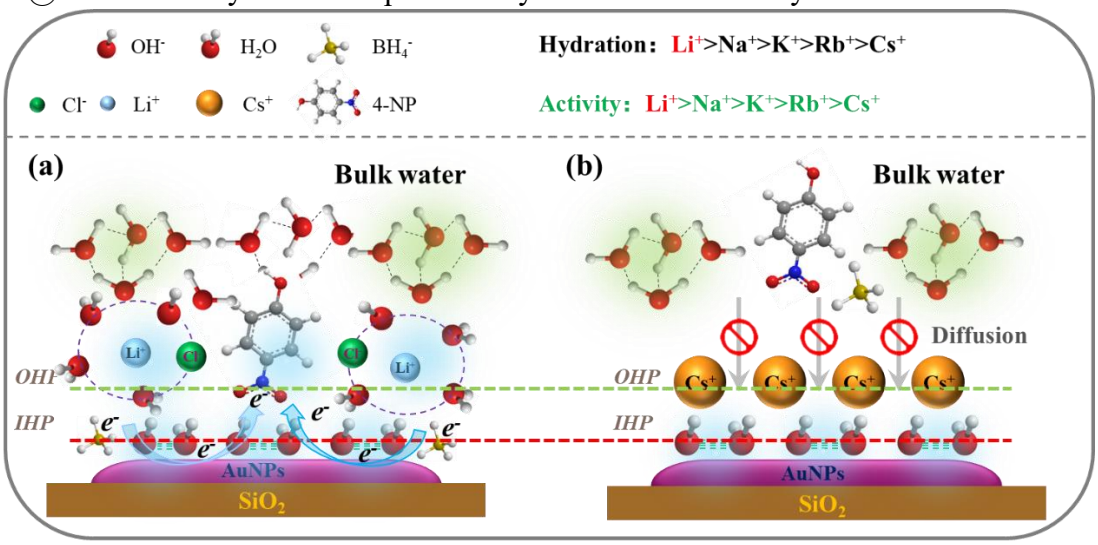

Scheme 1. Schematic illustration of the distribution of the reagent (4-NP and BH_4^-) and hydrated alkali-metal cations (AM^+, typical case of (a) Li^+ and (b) Cs^+) in the electrical double layer (EDL) region on the surface of gold NPs.[a] ([a]IHP represented inner Helmholtz plane, the structural water molecules (SW) in the form of ($OH^-{\cdot}H_2O$@Au NPs) are strongly adsorbed on the IHP; OHP represented outer Helmholtz plane, hydrated Li^+ and Cs^+ are attracted by the negatively charged surface of gold NPs at OHP. Li^+ cations with strong hydration capacity weakly bound on the Au NPs active site mainly plays two core roles in the reduction of 4-NP: on the one hand, acting as the relay (or gateway) station for water transportation (accelerating the proton transfer for the reduction of 4-NP); on the other hand, as an anchoring point of the counter-anion Cl^- by electrostatic interaction to optimize the molecular configuration of activated water by H-bonds, which accelerates the dissociation of O-H bond of water, and finally enhances reaction kinetics. While, for example, Cs^+ cations with a weak hydration ability strongly bind on the Au NPs, which blocks the diffusion of reaction substrate of BH_4^-, 4-NP and water to the active sites, thus slowing down the reaction rate of 4-NP reduction.)

attraction of alkali metal ions in the electrical double layer (EDL). Thus, the inner Helmholtz plane (IHP) of gold NPs is covered by SW with strong surface binding, while the outer Helmholtz plane (OHP) is filled with hydrated AM^+ cations (Scheme 1). The bulky Cs^+ cations with weak hydration capacity are strongly bound on the gold NPs surface due to the electrostatic interaction, which blocks the diffusion of reaction substrates (4-NP, water and BH_4^-) to the gold NPs active site and consequently lowers the reaction kinetics of the reduction of 4-NP. However, Li ions with strong hydration capacity are weakly adsorbed on the surface of Au nanoparticles due to charge shielding effect of the hydration shell, showing strong mobility, which not only does not affect the diffusion of the reaction substrate, but also can be used as the water relay or gateway station to provide activated hydrogen protons, thus accelerating the reaction kinetics. In addition, Cl^- as the counter-anion of Li^+ located around the catalytic active sites can stabilize the molecular configuration of activated water through H-bonds hydrogen bonding, thus accelerating the dissociation of O-H bonds of water molecules. Using this model, the kinetic isotope effects (KIEs) and the origin of hydrogen sources in the

reduction could be easily elucidated (Fig. 3), and also answer that the reduction of 4-NP does not follow the classical bimolecular L-H mechanism. In fact, the model of structural water as a bridge to transfer electron and proton in the confined nanospace is the reminiscent of working mechanism of photosystem two (PSII) for water splitting where Ca^{2+} and Cl^- also play the pivotal role to the activation of water on Mn_4CaO_5 cluster.[62-68]

Conclusion

In summary, with the hydride reduction of 4-NP as a benchmark or model reaction, we clearly elucidated the catalytic nature of Au active sites for electron and proton transfer at confined nanoscale interface. The composition of the catalytic active center includes not only the metal nanoparticles themselves, but also the structural water adsorbed on the surface of the metal nanoparticles. Different from the hydrogen bonding effect of bulk free water, due to the nano-confinement effect, the *p* orbitals of two oxygen atoms in the structural water adsorbed on Au NPs nanoparticles overlap to form an ensemble of interface electronic configurations by space interaction, which has the characteristics of π bonding.[39, 44, 45, 55, 60] These interface electronic states (the so-called PBIS state) provide the alternative channels for surface electron transfer. Because structural water (SW) participates in the construction of complex intermediate states (transition states), the long-range electron transfer between two reactants (BH_4^- and 4-NP) is extremely sensitive to the microenvironment of the catalytic active site. This also answers the two abnormal experimental phenomena observed by the isotope labelling experiment: the hydrogen of the final product 4-AP comes from water, not $NaBH_4$ reducer; the reaction kinetics of 4-NP reduction strongly depends on the type, concentration and counterions of alkali metal ions (AM^+). Herein, AM^+ and its counter-anions play a pivotal role of: (i) to stabilize the transition state of BH_4^--{OH^-·OH_2}-4-NP intermediate by H-Bonding interaction, which promotes the activation of O-H bond of water and concomitantly accelerates the cleavage of N-O bond of 4-NP. In fact, structural water plays a role as a media for electron transfer or exchange at nanoscale interface, which can be explained by the inner-coordination sphere electron transfer model of Marcus theory,[61] reminiscent of the working mechanism of the 'water bridge' or 'water line' for the electron and proton transfer in biological system, for example, photosystem II (PSII).[65-68] The model can also provide completely new insights into the understanding on the underlying mechanism of other redox reactions, which show similar pH- and cations-dependent or microenvironment-controlled catalytic activity, such as hydrogen evolution reaction (HER),[69-74] CO_2 and CO reduction,[75-78] low-temperature conversion of methane to methanol,[43, 79] water-gas shift reaction.[41, 42]

Acknowledgments

This research was funded by the National Key R&D Program of China (2021YFA1501401), the National Science Foundation of China (22172051, 21872053, and 21573074), the Science and Technology Commission of Shanghai Municipality (19520711400), the Research Funds of Happiness Flower ECNU (2020ST2203), the Open Project Program of Academician and Expert Workstation, Shanghai Curui Low-Carbon Energy Technology Co., Ltd., and the JORISS program. K.Z. thanks ENS de

Lyon for a temporary position as an invited professor in France.

Reference

[1] Wang C, Astruc D. Recent developments of nanocatalyzed liquid-phase hydrogen generation. *Chem. Soc. Rev.*, **2021**, 50: 3437-3484.

[2] Wang C, Wang Q, Fu F, et al. Hydrogen Generation upon Nanocatalyzed Hydrolysis of Hydrogen-Rich Boron Derivatives: Recent Developments. *Acc. Chem. Res.*, **2020**, 53: 2483-2493.

[3] Zhao P, Feng X, Huang D, et al. Basic concepts and recent advances in nitrophenol reduction by gold- and other transition metal nanoparticles. *Coord. Chem. Rev.*, **2015**, 287: 114-136.

[4] Hervés P, Pérez-Lorenzo M, Liz-Marzán L M, et al. Catalysis by metallic nanoparticles in aqueous solution: model reactions. *Chem. Soc. Rev.*, **2012**, 41: 5577.

[5] Zhang K, Suh J M, Choi J-W, et al. Recent Advances in the Nanocatalyst-Assisted NaBH4 Reduction of Nitroaromatics in Water. *ACS omega*, **2019**, 4: 483-495.

[6] Pradhan N, Pal A, Pal T. Silver nanoparticle catalyzed reduction of aromatic nitro compounds. *Colloids Surf. A Physicochem. Eng. Aspects*, **2002**, 196: 247-257.

[7] Wunder S, Polzer F, Lu Y, et al. Kinetic Analysis of Catalytic Reduction of 4-Nitrophenol by Metallic Nanoparticles Immobilized in Spherical Polyelectrolyte Brushes. *J. Phys. Chem. C*, **2010**, 114: 8814-8820.

[8] Wunder S, Lu Y, Albrecht M, et al. Catalytic Activity of Faceted Gold Nanoparticles Studied by a Model Reaction: Evidence for Substrate-Induced Surface Restructuring. *ACS Catal.*, **2011**, 1: 908-916.

[9] Antonels N C, Meijboom R. Preparation of Well-Defined Dendrimer Encapsulated Ruthenium Nanoparticles and Their Evaluation in the Reduction of 4-Nitrophenol According to the Langmuir−Hinshelwood Approach. *Langmuir*, **2013**, 29: 13433-13442.

[10] Kong X, Zhu H, Chen C, et al. Insights into the reduction of 4-nitrophenol to 4-aminophenol on catalysts. *Chem. Phys. Lett.*, **2017**, 684: 148-152.

[11] Zhao Y, Li R, Jiang P, et al. Mechanistic Study of Catalytic Hydride Reduction of −NO2 to −NH2 Using Isotopic Solvent and Reducer: The Real Hydrogen Source. *J. Phys. Chem. C*, **2019**, 123: 15582-15588.

[12] Shan B Q, Zhou J F, Ding M, et al. Surface electronic states mediate concerted electron and proton transfer at metal nanoscale interfaces for catalytic hydride reduction of -NO2 to -NH2. *Phys. Chem. Chem. Phys.*, **2021**, 23: 12950-12957.

[13] Ding M, Shan B-Q, Peng B, et al. Dynamic Pt–OH−·H2O–Ag species mediate coupled electron and proton transfer for catalytic hydride reduction of 4-nitrophenol at the confined nanoscale interface. *Phys. Chem. Chem. Phys.*, **2022**, 24: 7923-7936.

[14] Panigrahi S, Basu S, Praharaj S, et al. Synthesis and Size-Selective Catalysis by Supported Gold Nanoparticles: Study on Heterogeneous and Homogeneous Catalytic Process. *J. Phys. Chem. C*, **2007**, 111: 4596-4605.

[15] Dasog M, Hou W, Scott R W J. Controlled growth and catalytic activity of gold monolayer protected clusters in presence of borohydride salts. *Chem. Commun.*, **2011**, 47: 8569.

[16] Ciganda R, Li N, Deraedt C, et al. Gold nanoparticles as electron reservoir redox catalysts for 4-nitrophenol reduction: a strong stereoelectronic ligand influence. *Chem. Commun.*, **2014**, 50: 10126-10129.

[17] Ansar S M, Kitchens C L. Impact of Gold Nanoparticle Stabilizing Ligands on the Colloidal

Catalytic Reduction of 4-Nitrophenol. *ACS Catal.*, **2016**, 6: 5553-5560.

[18] Roy S, Rao A, Devatha G, et al. Revealing the Role of Electrostatics in Gold-Nanoparticle-Catalyzed Reduction of Charged Substrates. *ACS Catal.*, **2017**, 7: 7141-7145.

[19] Zhuang Q, Yang Z, Sobolev Y I, et al. Control and Switching of Charge-Selective Catalysis on Nanoparticles by Counterions. *ACS Catal.*, **2018**, 8: 7469-7474.

[20] Lin C, Tao K, Hua D, et al. Size Effect of Gold Nanoparticles in Catalytic Reduction of p-Nitrophenol with NaBH4. *Molecules*, **2013**, 18: 12609-12620.

[21] Kastner C, Thünemann A F. Catalytic Reduction of 4-Nitrophenol Using Silver Nanoparticles with Adjustable Activity. *Langmuir*, **2016**, 32: 7383-7391.

[22] Menumerov E, Hughes R A, Golze S D, et al. Identifying the True Catalyst in the Reduction of 4‑Nitrophenol: A Case Study Showing the Effect of Leaching and Oxidative Etching Using Ag Catalysts. *ACS Catal.*, **2018**, 8: 8879-8888.

[23] Neal R D, Hughes R A, Sapkota P, et al. Effect of Nanoparticle Ligands on 4-Nitrophenol Reduction: Reaction Rate, Induction Time, and Ligand Desorption. *ACS Catal.*, **2020**, 10: 10040-10050.

[24] Yang T-Q, Ning T-Y, Peng B, et al. Interfacial electron transfer promotes photo-catalytic reduction of 4-nitrophenol by Au/Ag_2O nanoparticles confined in dendritic mesoporous silica nanospheres. *Catal. Sci. Technol.*, **2019**, 9: 5786-5792.

[25] Menumerov E, Hughes R A, Neretina S. Catalytic Reduction of 4-Nitrophenol: A Quantitative Assessment of the Role of Dissolved Oxygen in Determining the Induction Time. *Nano Lett.*, **2016**, 16: 7791-7797.

[26] Wang C, Zou W, Wang J, et al. Insight into the mechanism of gold-catalyzed reduction of nitroarenes based on the substituent effect and in situ IR. *New J. Chem.*, **2017**, 41 3865-3871.

[27] Grzeschik R, Schäfer D, Holtum T, et al. On the Overlooked Critical Role of the pH Value on the Kinetics of the 4-Nitrophenol NaBH4-Reduction Catalyzed by Noble-Metal Nanoparticles (Pt, Pd, and Au). *J. Phys. Chem. C*, **2020**, 124: 2939-2944.

[28] Shirin S, Roy S, Rao A, et al. Accelerated Reduction of 4-Nitrophenol: Bridging Interaction Outplays Reducing Power in the Model Nanoparticle-Catalyzed Reaction. *J. Phys. Chem. C*, **2020**, 124: 19157-19165.

[29] Strachan J, Barnett C, Masters A F, et al. 4-Nitrophenol Reduction: Probing the Putative Mechanism of the Model Reaction. *ACS Catal.*, **2020**, 10: 5516-5521.

[30] Hu X-D, Shan B-Q, Tao R, et al. Interfacial Hydroxyl Promotes the Reduction of 4-Nitrophenol by Ag-based Catalysts Confined in Dendritic Mesoporous Silica Nanospheres. *J. Phys. Chem. C*, **2021**, 125: 2446-2453.

[31] Swathy T S, Antony M J, George N. Active Solvent Hydrogen-Enhanced p-Nitrophenol Reduction Using Heterogeneous Silver Nanocatalysts@Surface-Functionalized Multiwalled Carbon Nanotubes. *Ind. Eng. Chem. Res.*, **2021**, 60: 7050-7064.

[32] Kong X-k, Sun Z-y, Chen M, et al. Metal-free catalytic reduction of 4-nitrophenol to 4-aminophenol by N-doped graphene. *Energy Environ. Sci.*, **2013**, 6: 3260.

[33] Roy A, Debnath B, Sahoo R, et al. Micelle confined mechanistic pathway for 4-nitrophenol reduction. *J. Colloid Interface Sci.*, **2017**, 493: 288-294.

[34] Yu Y J, Xing J L, Pang J L, et al. Facile synthesis of size controllable dendritic mesoporous silica nanoparticles. *ACS Appl. Mater. Interfaces*, **2014**, 6: 22655-22665.

[35] Zhang K, Xu L L, Jiang J G, et al. Facile large-scale synthesis of monodisperse mesoporous

silica nanospheres with tunable pore structure. *J. Am. Chem. Soc.*, **2013**, 135: 2427-2430.

[36] Liu P C, Yu Y J, Peng B, et al. A dual-templating strategy for the scale-up synthesis of dendritic mesoporous silica nanospheres. *Green Chem.*, **2017**, 19: 5575-5581.

[37] Peng B, Zong Y-X, Nie M-Z, et al. Interfacial Charge Shielding Directs Synthesis of Dendritic Mesoporous Silica Nanospheres by a Dual-Templating Approach. *New J. Chem.*, **2019**, 43: 15777-15784.

[38] Hao P, Peng B, Shan B-Q, et al. Comprehensive understanding of the synthesis and formation mechanism of dendritic mesoporous silica nanospheres. *Nanoscale Adv.*, **2020**, 2: 1792-1810.

[39] Peng B, Zheng L-X, Wang P-Y, et al. Physical Origin of Dual-Emission of Au–Ag Bimetallic Nanoclusters. *Front. Chem.*, **2021**, 9: 756993.

[40] Zheng L-X, Peng B, Zhou J-F, et al. High efficient and stable thiol-modified dendritic mesoporous silica nanospheres supported gold catalysts for gas-phase selective oxidation of benzyl alcohol with ultra-long lifetime. *Microporous Mesoporous Mater.*, **2022**, 342: 112140.

[41] Yang M, Li S, Wang Y, et al. Catalytically active Au-O(OH)x-species stabilized by alkali ions on zeolites and mesoporous oxides. *Science*, **2014**, 346: 1498-1501.

[42] Zhai Y, Pierre D, Si R, et al. Alkali-Stabilized Pt-OHx Species Catalyze Low-Temperature Water-Gas Shift Reactions. *Science*, **2010**, 329: 1633-1636.

[43] Liu Z, Huang E, Orozco I, et al. Water-promoted interfacial pathways in methane oxidation to methanol on a CeO2-Cu2O catalyst. *Science*, **2020**, 368: 513-517.

[44] Yang T-Q, Hu X-D, Shan B-Q, et al. Caged structural water molecules emit tunable brighter colors by topological excitation. *Nanoscale*, **2021**, 13: 15058-15066.

[45] Zhou J, Yang T, Peng B, et al. Structural Water Molecules Confined in Soft and Hard Nanocavities as Bright Color Emitters. *ACS Phys. Chem. Au*, **2022**, 2: 47-58.

[46] Wang P-Y, Zhou J-F, Chen H, et al. Activation of H_2O Tailored by Interfacial Electronic States at a Nanoscale Interface for Enhanced Electrocatalytic Hydrogen Evolution. *JACS Au*, **2022**, 2: 1457-1471.

[47] Yang T, Zhou J, Shan B, et al. Hydrated Hydroxide Complex Dominates the AIE Properties of Nonconjugated Polymeric Luminophores. *Macromol. Rapid Commun.*, **2022**, 43: 2100720.

[48] Kollonitsch J, Fuchs O, GÁBor V. Alkaline-Earth Borohydrides and their Applications in Organic Syntheses. *Nature*, **1955**, 175: 346-346.

[49] Brown H C, Rao B C S. A New Powerful Reducing Agent-Sodium Borohydride in the Presence of Aluminum Chloride and Other Polyvalent Metal Halides. *J. Am. Chem. Soc.*, **1956**, 78: 2582-2588.

[50] Brown H C, Narasimhan S, Choi Y M. Effect of cation and solvent on the reactivity of saline borohydrides for reduction of carboxylic esters. Improved procedures for the conversion of esters to alcohols by metal borohydrides. *J. Org. Chem.*, **1982**, 47: 4702-4708.

[51] Marcus Y. Effect of Ions on the Structure of Water: Structure Making and Breaking. *Chem. Rev.*, **2009**, 109: 1346-1370.

[52] Nihonyanagi S, Yamaguchi S, Tahara T. Counterion Effect on Interfacial Water at Charged Interfaces and Its Relevance to the Hofmeister Series. *J. Am. Chem. Soc.*, **2014**, 136: 6155-6158.

[53] Chen Y, Yang T, Pan H, et al. Photoemission Mechanism of Water-Soluble Silver Nanoclusters: Ligand-to-Metal–Metal Charge Transfer vs Strong Coupling between Surface Plasmon and Emitters. *J. Am. Chem. Soc.*, **2014**, 136: 1686-1689.

[54] Yang T, Dai S, Yang S, et al. Interfacial Clustering-Triggered Fluorescence–Phosphorescence

Dual Solvoluminescence of Metal Nanoclusters. *J. Phys. Chem. Lett.*, **2017**, 8: 3980-3985.

[55] Yang T, Shan B, Huang F, et al. P band intermediate state (PBIS) tailors photoluminescence emission at confined nanoscale interface. *Commun. Chem.*, **2019**, 2: 1-11.

[56] Yang T-Q, Peng B, Shan B-Q, et al. Origin of the Photoluminescence of Metal Nanoclusters: From Metal-Centered Emission to Ligand-Centered Emission. *Nanomaterials*, **2020**, 10: 261.

[57] Tao R, Shan B-Q, Sun H-D, et al. Surface Molecule Manipulated Pt/TiO2 Catalysts for Selective Hydrogenation of Cinnamaldehyde. *J. Phys. Chem. C*, **2021**, 125: 13304-13312.

[58] Ewles J. Water as an Activator of Luminescence. *Nature*, **1930**, 125: 706-707.

[59] Przibram K. Fluorescence of Adsorbed Water. *Nature*, **1958**, 182: 520-520.

[60] Hoffmann R. Interaction of orbitals through space and through bonds. *Acc. Chem. Res.*, **1971**, 4: 1-9.

[61] Kellett C W, Swords W B, Turlington M D, et al. Resolving orbital pathways for intermolecular electron transfer. *Nat. Commun.*, **2018**, 9: 1-10.

[62] Duan L, Fischer A, Xu Y, et al. Isolated Seven-Coordinate Ru(IV) Dimer Complex with [HOHOH]- Bridging Ligand as an Intermediate for Catalytic Water Oxidation. *J. Am. Chem. Soc.*, **2009**, 131: 10397-10399.

[63] Young I D, Ibrahim M, Chatterjee R, et al. Structure of photosystem II and substrate binding at room temperature. *Nature*, **2016**, 540: 453-457.

[64] Barber J. Photosynthetic Water Splitting Provides a Blueprint for Artificial Leaf Technology. *Joule*, **2017**, 1: 5-9.

[65] Barber J. 'Photosystem II: the water splitting enzyme of photosynthesis and the origin of oxygen in our atmosphere'. *Q. Rev. Biophys.*, **2016**, 49.

[66] Barber J. A mechanism for water splitting and oxygen production in photosynthesis. *Nat. Plants*, **2017**, 3: DOI: 10.1038/nplants.2017.1041.

[67] Kern J, Chatterjee R, Young I D, et al. Structures of the intermediates of Kok's photosynthetic water oxidation clock. *Nature*, **2018**, 563: 421-425.

[68] Suga M, Akita F, Yamashita K, et al. An oxyl/oxo mechanism for oxygen-oxygen coupling in PSII revealed by an x-ray free-electron laser. *Science*, **2019**, 366: 334-338.

[69] Wang Y-H, Zheng S, Yang W-M, et al. In situ Raman spectroscopy reveals the structure and dissociation of interfacial water. *Nature*, **2021**, 600: 81-85.

[70] Huang B, Rao R R, You S, et al. Cation- and pH-Dependent Hydrogen Evolution and Oxidation Reaction Kinetics. *JACS Au*, **2021**, 1: 1674-1687.

[71] Liu E, Li J, Jiao L, et al. Unifying the Hydrogen Evolution and Oxidation Reactions Kinetics in Base by Identifying the Catalytic Roles of Hydroxyl-Water-Cation Adducts. *J. Am. Chem. Soc.*, **2019**, 141: 3232-3239.

[72] Zheng J, Sheng W, Zhuang Z, et al. Universal dependence of hydrogen oxidation and evolution reaction activity of platinum-group metals on pH and hydrogen binding energy. *Sci. Adv.*, **2016**, 2: e1501602.

[73] Strmcnik D, Kodama K, Vliet D v d, et al. The role of non-covalent interactions in electrocatalytic fuel-cell reactions on platinum. *Nat. Chem.*, **2009**, 1: 466-472.

[74] Ledezma-Yanez I, Wallace W D Z, Sebastián-Pascual P, et al. Interfacial water reorganization as a pH-dependent descriptor of the hydrogen evolution rate on platinum electrodes. *Nat. Energy*, **2017**, 2: 17031.

[75] Singh M R, Kwon Y, Lum Y, et al. Hydrolysis of Electrolyte Cations Enhances the

Electrochemical Reduction of CO_2 over Ag and Cu. *J. Am. Chem. Soc.*, **2016**, 138: 13006-13012.

[76] Pérez-Gallent E, Marcandalli G, Figueiredo M C, et al. Structure- and Potential-Dependent Cation Effects on CO Reduction at Copper Single-Crystal Electrodes. *J. Am. Chem. Soc.*, **2017**, 139: 16412-16419.

[77] Resasco J, Chen L D, Clark E, et al. Promoter Effects of Alkali Metal Cations on the Electrochemical Reduction of Carbon Dioxide. *J. Am. Chem. Soc.*, **2017**, 139: 11277-11287.

[78] Yu S, Louisia S, Yang P. The Interactive Dynamics of Nanocatalyst Structure and Microenvironment during Electrochemical CO_2 Conversion. *JACS Au*, **2022**, 2: 562-572.

[79] Zuo Z, Ramírez P J, Senanayake S D, et al. Low-Temperature Conversion of Methane to Methanol on CeO_x/Cu_2O Catalysts: Water Controlled Activation of the C-H Bond. *J. Am. Chem. Soc.*, **2016**, 138: 13810-13813.

Graphic abstract (GA) and TOC

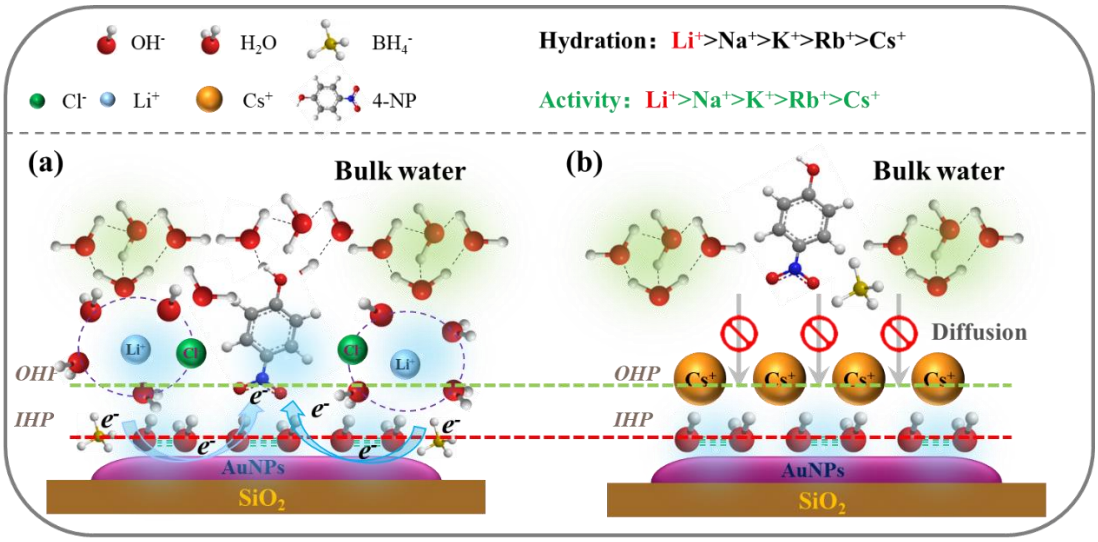

The structural water molecules (SW) absorbed on Au nanoparticles in the form of {$OH^-·H_2O$@Au NPs} were identified as catalytic active sites for the reduction of 4-NP (not alone Au NPs), where the overlapping of the *p* orbital of oxygen atoms of the hydroxyl (hydroxide) groups and water molecules in SW by space interaction yields an ensemble of interfacial electronic states, which synergistically promotes both interfacial electron transfer and the activation of water (dissociation of O-H bonds) or proton transfer.